Features and Formation Mechanism of the Jiaopenba Landslide, Southwestern Sichuan Province, China

Tong Shen[1,2]*, Yunsheng Wang[2]*, Xun Zhao[2], Heng Liu[1], Xuyang Wu[1], Yapei Chu[1], Panpan Zhai[1] and Yang Han[1]

[1]Henan University of Urban Construction, School of Civil Engineering, Pingdingshan, China, [2]State Key Laboratory of Geohazard Prevention and Geoenvironment Protection, Chengdu University of Technology, Chengdu, China

The Jiaopenba landslide, which represents a typical large basalt high-speed remote landslide, is located in Emeishan City, southwestern Sichuan province, China. Based on the field investigation, the characteristics of the Jiaopenba landslide have been revealed. The Jiaopenba landslide occurred on the steep Mount Emei. Landslide materials with a volume of approximately 6.75×10^8 m^3 slid down from a high position, forming a large-scale high-speed remote debris flow, with the farthest sliding distance of about 7.5 km. The landslide area is located in the west wing of the Emeishan anticline, which is cut by faults to form a monoclinal fault-block mountain. Although the shear outlet of the landslide is near the slope toe and does not have good free conditions, there are faults passing through the slope toe of the bedding slope of the fault hanging wall, the landslide is affected by the fault activity, and the integrity of the layered slope is poor. When the foot of the slope is empty, the fault zone is compressed and plastic extrusion, which leads to bedding slip of the slope rock mass and greatly weakens the interlayer bonding force. When coupled with long structural planes on both sides to form side crack planes, a large-scale inclined plate structure is formed. Under the action of a strong earthquake and other external forces, the rock mass near the fault can be damaged by tension, and a large-scale high-position landslide can be formed by the mode of compression-slip-tension fracture.

Keywords: Jiaopenba landslide, Emeishan basalt, earthquake-induced paleolandslide, high-speed remote landslide, formation mechanism

HIGHLIGHTS

1 The Jiaopenba landslide occurred on the steep Mount Emei, with a volume of approximately 6.75×10^8 m^3 slid down from a high position along a surface formed by weak intercalation of volcanic agglomerate and breccia, and the farthest sliding distance reached about 7.5 km.

2 Due to the accumulation of landslide materials and the erosion and undercutting of rivers in the later stage, the platform terrain separated by the river valley formed the fifth level planation plane in the study area (elevation: 900–1,000 m). Through the comparative analysis of regional plantation levels and combined with the research results of Valley evolution in Dadu River Basin, it can be judged that the landslide was roughly formed in the Middle Pleistocene.

3 The occurrence of landslide needs to go through three stages: deformation accumulation stage, triggering instability stage, and sliding failure stage.

4 Jiaopenba landslide developed in the hanging wall of the fault. The landslide is affected by fault activity, and the integrity of the layered slope is poor. When the foot of the slope was empty, the fault zone was compressed and plastically extruded, which led to bedding slip of the slope rock mass and greatly weakened the interlayer bonding force. When coupled with long structural planes on both sides to form side crack planes, a large-scale inclined plate structure was formed. Under the action of a strong earthquake, the rock mass near the fault can undergo tensile failure, forming a large high-position landslide in the mode of compression-slip-tension fracture.

5 The investigation shows that the Emeishan basalt debris flow is mainly composed of coarse-grained rocks. In the process of motion, large particles often collide with each other, with obvious momentum transfer. In addition, the basalt debris particles with a higher degree of fracture have better particle sphericity, and particles with good sphericity are prone to bounce and roll during movement. Under this movement mode, the effective friction coefficient between particles and the sliding surface is lower and has a momentum transfer effect during the movement. The combination of factors makes the landslide debris flow maintain a higher speed and a longer distance.

INTRODUCTION

Widely distributed Permian-age basalts throughout Southwest China are often selected as ideal sites for large hydropower projects because of their huge thick layer structure, high strength, and formation of a canyon landform (Wei, 2007; Han, 2015; Shen et al., 2019a). Another remarkable feature of Emeishan basalt is that they are composed of multiple overflow cycles with weak intercalations such as tuff, volcanic agglomerate, and breccia (Xu, 2010; Sun, 2011). Although Emeishan basalt has high strength and a huge thick layer structure, the slope rock mass is generally stable. However, basalt has special lithologic characteristics and mechanical properties of the rock mass. Once the high-level basaltic rock mass with huge potential energy loses stability, it can develop into a high-speed and long-runout giant landslide disaster (Xu, 2010; Tian, 2015; Wei, 2016; Yang, 2017; Wen, 2021). Related studies have shown that Emeishan basalt is a special rock series that can breed large-scale high-position and long-distance landslide disasters (Shen, 2019). In history, such landslides have caused a lot of casualties, property losses, and far-reaching environmental effects. For example, on 23 November 1965, one such basalt landslide occurred in Lannigou, Yunnan province: five villages were buried and caused 444 deaths. Another basalt landslide struck Touzhai, in Zhaotong City, Yunnan province, on 23 September 1991, and 216 people were killed. On 27 July 2010, a large basalt landslide near Ermanshan, Hanyuan city in Sichuan province: buried 20 people, damaged 97 houses, and forced 1,500 people to be transferred.

Why do so many catastrophic landslides occur along basalt slopes, and what is the formation mechanism of these landslides? This study aims to solve these problems. Jiaopenba landslide is a typical large basalt high-speed remote landslide event. Based on the detailed geological survey, combined with remote sensing interpretation data, laboratory test, the characteristics, failure mechanism, and movement processes of the landslide are studied.

REGIONAL GEOLOGICAL SETTING

The landslide area is located in the west wing of the Emeishan anticline in the Daeshan fault block cut by the Emeishan, Xinkaisi, Wanniansi, and Maziba faults (**Figure 1**). Granites of the Pre-Sinian System constitute the core of the Emeishan anticline, and the Sinian, Cambrian, Ordovician, Permian, and Triassic strata respectively constitute the two wings of the anticline.

Since the Middle Pleistocene, affected by the tectonic stress in the west, the Emeishan area has been strongly uplifted many times, accompanied by strong and frequent seismicity (Wang et al., 2013). The seismic intensity of the study area is degree VII.
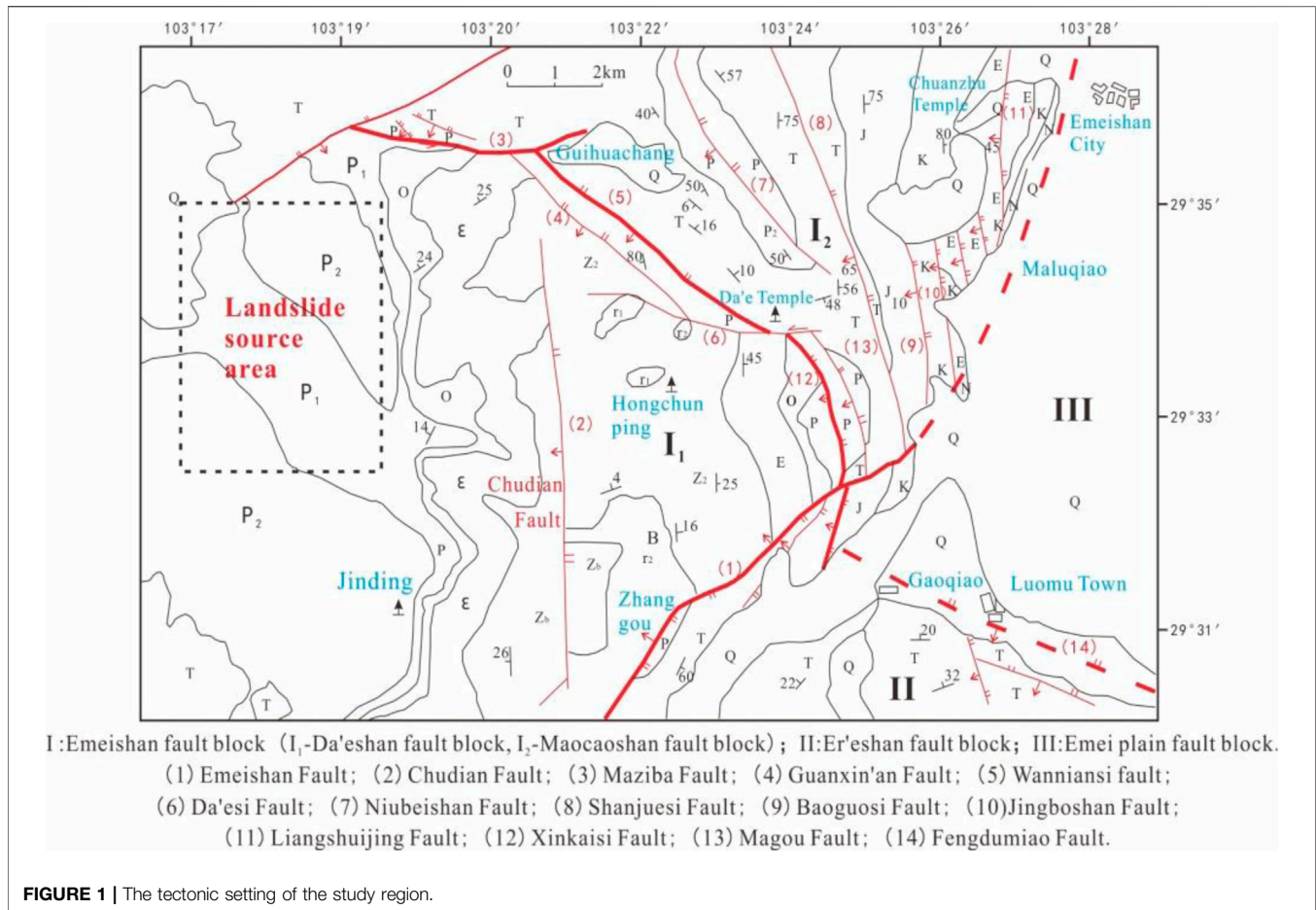
The landslide is located in the Jiaopenba area, Emeishan City, Sichuan province, China, which is generally distributed as a strip in the northwest direction (**Figure 2**). The back edge of the landslide area is located in Leidongping (elevation: 2,340 m), and the front edge of the landslide area is distributed in Nanmuping (elevation: 830 m). The height difference between the back and front edges of the landslide area is 1,510 m.

According to the integrated geological investigation, there are faults (**Figure 3**) passing through the shearing surface of the landslide (the elevation distribution of the faults is mainly exposed in the range of 1,320–1,350 m), and the landslide is located at the hanging wall of the fault. The fault strike extends toward the northeast, and the fracture surface leans to the southeast, with a dip angle of 60˚–70˚, which belongs to the branch fault of the Maziba fault. The fault is mainly translational and also shows the nature of the reverse fault. The west segment of the fault is covered by Quaternary materials.

Shihe River flows from the south to the north through the front edge of the landslide source area (**Figures 2**, **3**). It originates from the Wanfoding and Jieyindian areas of Emei Mountain. Due to the continuous undercutting and erosion of the slope toe by the river, an open valley landform is formed in the front of the slope. The exposed strata in the study area are mainly basalts of the Upper Permian Emeishan Formation ($P_2\beta$), which formed the landslide source (**Figure 3**). The basalts are underlain by limestone of the Lower Permian Yangxin Formation (P_1Y) and overlain by sandstones of the Lower Triassic Feixianguan Formation (T_1f), which primarily are exposed along both banks of the Shihe Valley.

CHARACTERISTICS OF THE LANDSLIDE

Based on field investigation, combined with the movement evolution process, the material composition, and structural

I :Emeishan fault block (I₁-Da'eshan fault block, I₂-Maocaoshan fault block) ; II:Er'eshan fault block; III:Emei plain fault block.
(1) Emeishan Fault; (2) Chudian Fault; (3) Maziba Fault; (4) Guanxin'an Fault; (5) Wanniansi fault;
(6) Da'esi Fault; (7) Niubeishan Fault; (8) Shanjuesi Fault; (9) Baoguosi Fault; (10)Jingboshan Fault;
(11) Liangshuijing Fault; (12) Xinkaisi Fault; (13) Magou Fault; (14) Fengdumiao Fault.

FIGURE 1 | The tectonic setting of the study region.

characteristics of the landslide, the landslide area was subdivided into a conflux area (I), source area (II), transportation area (III), and accumulation area (IV).

Conflux Area

The conflux area of the landslide is distributed in the upper part of the landslide source area, with an elevation range of 2,350–3,099 m. Because the upper part of the rear edge of the landslide is a flat planation surface, the stratigraphic dip angle in the Jinding area is 10°–20°, which can form a large catchment section. The area has abundant precipitation, developed bedrock fissures, and good penetration. With rainfall, snow infiltration, and groundwater runoff along the layer, the water continuously converges at the trailing edge of the landslide (**Figures 2**, **3**).

Layered fissures and columnar joints are developed in Emeishan Basaltic rock mass, which provides channels for the seepage of atmospheric precipitation and surface water. Groundwater is mostly active in rock strata with pore structure and columnar joints. The tuff interlayer in basalt has poor water permeability and becomes a relatively impermeable layer, forming a bedrock fissure aquifer. Field investigation reveals that spring water is exposed near Leidongping (elevation 2,340 m) below the confluence area (**Figure 4**), and

obvious corrosion can be seen in the bedrock exposed near the spring.

Landslide Source Area

The landslide source area is located in the west wing of the Emeishan anticline, which is cut by faults to form a monoclinal bedding slope. In terms of overall topography, the middle and lower parts of the slope are relatively steep due to the influence of fold structure, the slope is moderately inclined (the stratum dip angle is 30°–35°), and the elevation at the foot of the mountain is 1,300 m. The slope tends to be gentle toward the upper part, the elevation of the trailing edge of the landslide source area is 2,500 m, and the height difference between the top and the foot of the mountain in the source area is 1,200 m (**Figure 5**).

After the landslide occurrence, a huge groove topography was formed in the source area (**Figures 2**, **5**). A large area of smooth bedding plane of limestone of Lower Permian Yangxin Formation (P_1y) is exposed in the landslide source area, parts of the unslided Emeishan Basaltic Rocks still exist at the trailing edge of the source area (**Figure 3**), which have strong weathering and unloading, and joint fissures are developed. The bedrock attitude in the source area is 306° ∠35°, which generally shows a medium dip bedding slope. The original slope of the rock mass
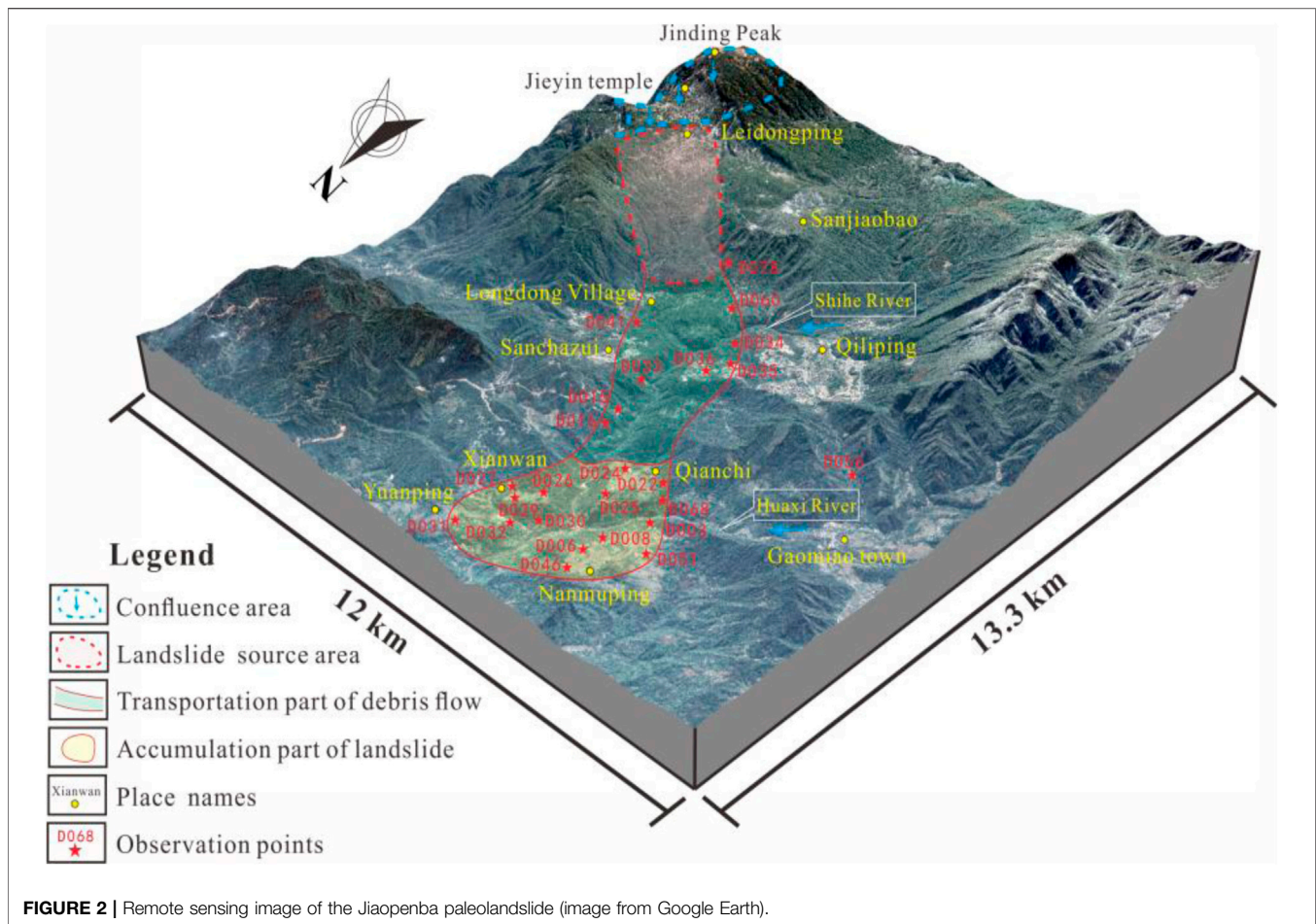
FIGURE 2 | Remote sensing image of the Jiaopenba paleolandslide (image from Google Earth).

is about 40°, the overall sliding direction is 319°, and the sliding volume is about $6.75 \times 10^8 \, \text{m}^3$.

Transportation Area

After the landslide slid out of the shear outlet, a large amount of landslide materials moved rapidly along the Shihe valley toward the NW direction, forming a high-speed remote debris flow with rapid disintegration (**Figure 2**).

The sliding range of the circulation area is about 5 km. The elevation of the rear edge of the circulation area is about 1,400 m, the front edge is about 900 m, and the height difference is 500 m. The terrain of the circulation area is relatively gentle, with a gradient of about 10°–15°, and there are two-stage scarps (**Figure 2**). In the process of high-speed movement, the debris flow strongly scraped the loose materials on the surface of the main ditch bed. Due to the energy consumption caused by gentle terrain change and scraping, some landslide materials scattered and accumulated in the ditch and both sides of the ditch, whereas those with greater energy continued to move with the scraped materials.

A large number of fractured stones and boulders, mostly basalt mixed with sandstone, are widely distributed throughout this area (**Figure 2**). The particle size is generally 2–20 cm, and clasts are mostly angular; the basaltic gravels are highly weathered, and some show severe argillization. The basaltic stones were mainly

amygdaloidal and massive, and a large amount of sandstone was also mixed into the deposits, proving that the landslide materials scraped and collided with the mountain, after which massive bedrock materials were carried within the flow. Some larger basaltic boulders with a generally amygdaloidal structure, with maximum dimensions of $7 \times 5 \times 3 \, \text{m}^3$ (**Figure 6**), were distributed along this area (observation points D060, D041, D034, D033, D016, and D036).

The accumulation body distributed in the landslide transportation area has the accumulation characteristics of inverse grading structure: the upper part of the landslide accumulation body contains more large-sized boulders, whereas the lower part contains fewer boulders, mainly small particles such as gravel and breccia (**Figure 7**). Bedrock is exposed near survey point D015 (4 km away from the landslide source area) (**Figure 7**), and the lithology is sandstones of the Upper Triassic Xujiahe Formation (T_3x). Scratches can be seen on the rock mass surface, formed by scraping the bedrock with landslide materials (**Figure 7**). The scratches point downstream along the valley, indicating the movement direction of landslide materials (320°).

Accumulation Areas

After a long distance of landslide material movement, it gradually entered the accumulation stage due to the change of terrain and the

FIGURE 3 | Geomorphological sketch map of the Jiaopenba paleolandslide area.
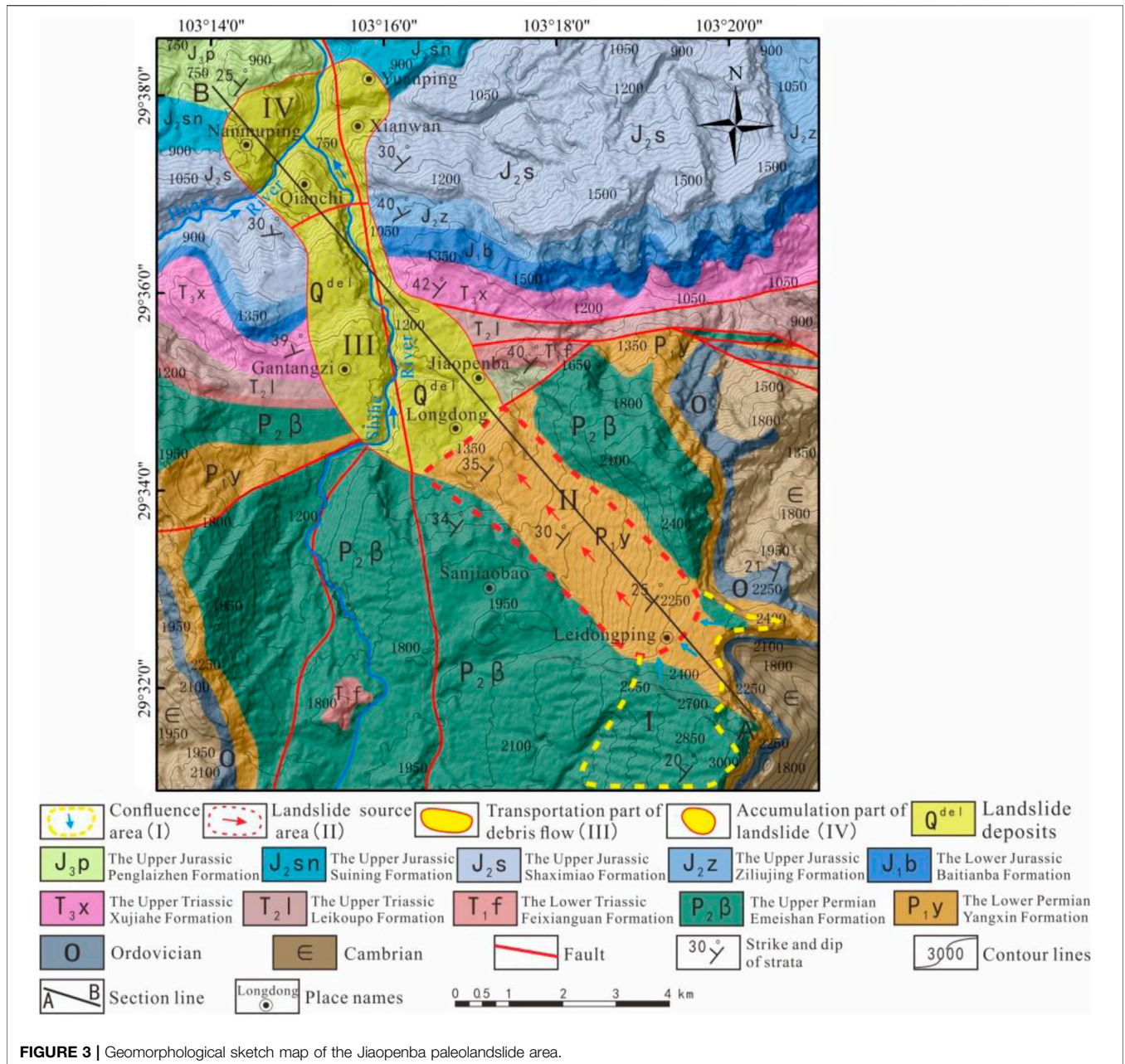
gradual dissipation of energy. The accumulation area is mainly distributed in the areas of Qianchi (**Figure 8**), Xianwan, Yuanping, and Nanmuping. Because of the accumulation of landslide materials and the erosion of the river in the later stage, the platform terrain separated by the river valley formed in the accumulation area (**Figures 2**, **3**). Due to the long-term erosion and undercutting of the landslide accumulation by the river, a good section that can reveal the internal structure and material composition of the accumulation can be displayed.

This area is covered with landslide deposits mainly composed of soil with massive gravel- and boulder-sized clasts. The gravels were highly weathered with mostly sub-angular clasts with a particle size of 0.5–10 cm and a maximum diameter of 20 cm; their structure was

disordered and dense, with mainly argillaceous and some calcareous cementation and some show severe argillization. Most of the gravels are basalt mixed with sandstone and dolomite (**Figures 8**, **9**), proving that the landslide materials scraped and collided with the mountain, after which massive bedrock materials were carried within the flow. Some larger basaltic boulders with a generally amygdaloidal structure, with volumes up to 10 m³, were distributed along this area (**Figures 8**, **9**).

A good profile of landslide deposits (**Figure 9**), 76 m high, at observation point D032 (elevation: 770 m), exposes the internal structure of the debris deposit. The landslide deposits here are mainly composed of soil with massive basalt gravels and boulders. These gravels, which have mostly 0.2–5 cm angular clasts (18 cm

FIGURE 4 | Spring is exposed near Leidongping below the confluence area **(A)** The distant view. (**(B)** Dissolution grooves are developed in limestone).
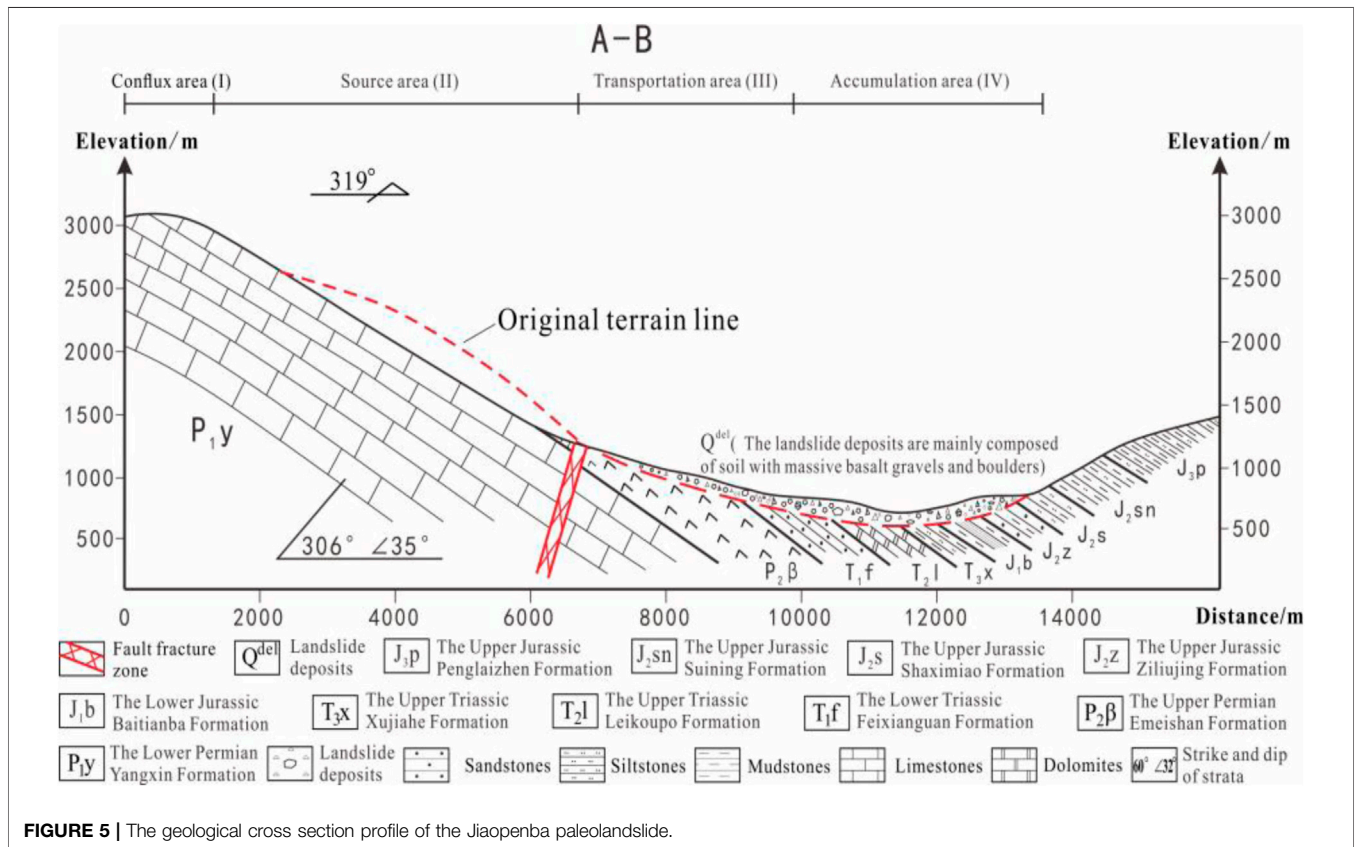

FIGURE 5 | The geological cross section profile of the Jiaopenba paleolandslide.

maximum diameter) of amygdaloidal and massive basalt, mixed with sandstone and dolomite, are chaotically arranged with compact cementation, and some show severe argillization. At different heights of the vertical section, the internal structure of the debris deposit also has the accumulation characteristics of an inverse grading structure.

Observation point D051 (elevation: 770 m) is located on the platform of Nanmuping village and belongs to the front edge of

landslide accumulation. There is a good profile of landslide deposits exposed here (**Figure 10**), and the landslide materials were mainly composed of soil with massive basaltic gravel- and boulder-sized clasts (**Figure 10**). The gravels were highly weathered with mostly sub-angular clasts with a particle size of 0.2–10 cm and a maximum diameter of 20 cm; their structure was disordered and dense, with mainly argillaceous and some calcareous cementation. The basaltic stones were mainly
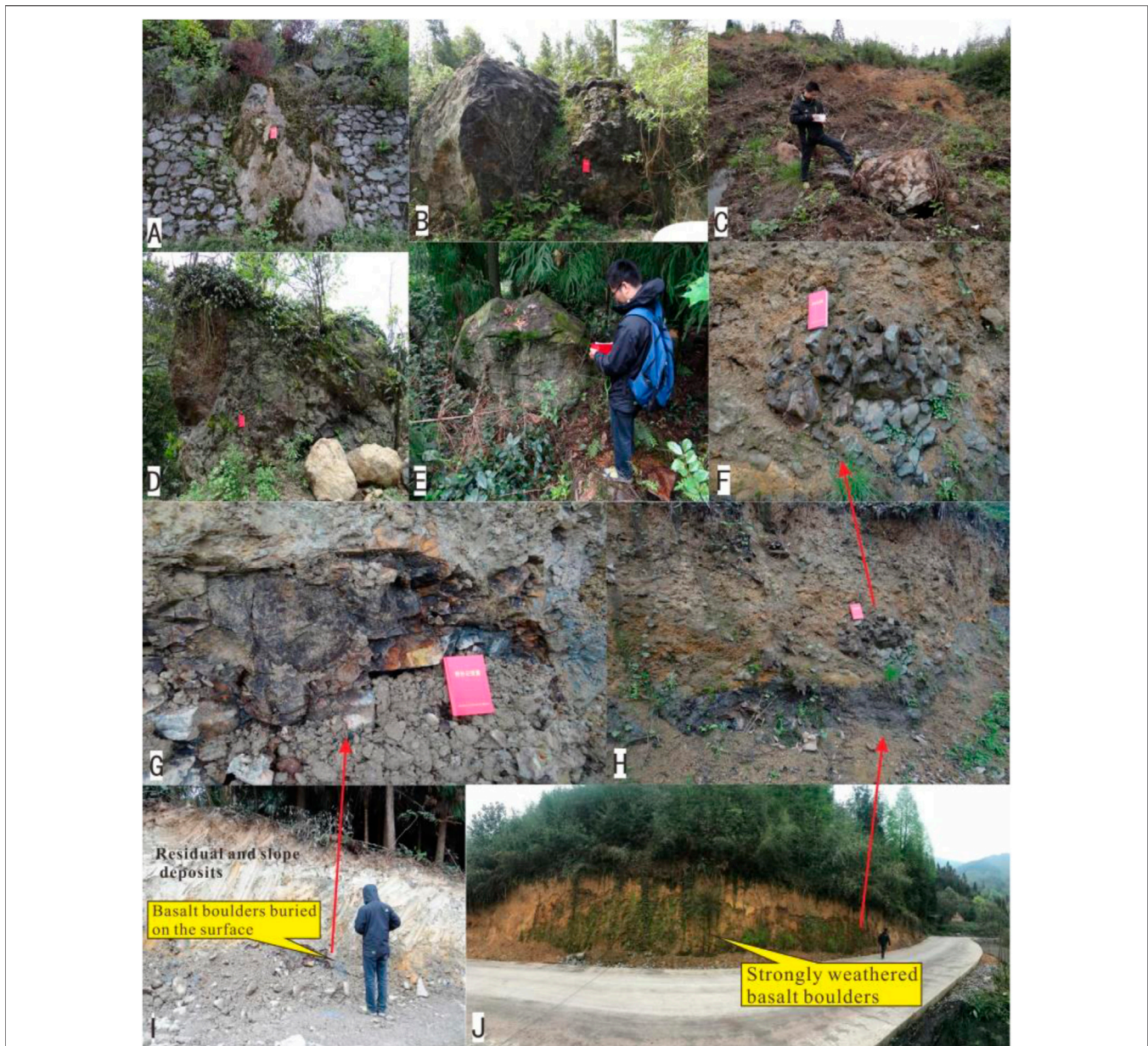
FIGURE 6 | Basalt boulders widely distributed in the landslide transportation area. **(A,B,C,D,E)** Basalt boulders distributed at observation points D060, D041, D034, D033, and D016, respectively. **(G,I)** Basalt boulders buried on the surface can be seen at observation point D035 (seriously weathered and show severe argillization). **(F,H,J)** Massive basalt boulders and gravels exposed at the observation point D036.

amygdaloidal and massive, and a large amount of dolomites were also mixed into the deposits, proving that the front of landslide debris flow scraped and collided with the mountain and carried the Dolomites of the Triassic Leikoupo Formation along the way. In addition, basaltic boulders are distributed around the survey site, and some show severe argillization. The saprolite crusts from chemical weathering occurring along discontinuity surfaces and enclosing the inner fresher core stone made the rock mass evolve into the structure of soil sandwiching rock (**Figure 10**). This "soil sandwiching rock" structure is more common in the seriously weathered basalt (Xu, 2005; Wang, 2013; Zhang, 2017).

The landslide finally blocked the Shihe River and formed a landslide dam. The upper parts of Nanmuping, Yuanping, Xianwan, and Qianchi are platform topography, forming a complete ancient landslide dam body, which were cut by rivers and separated from each other so that the material composition inside the accumulation body can be shown. According to the investigation results of the distribution of landslide deposits and the interface deposits front base cover, it is inferred that the accumulation thickness of the ancient landslide dam is about 150 m, and the total volume of landslide accumulation is about $3.7 \times 10^8 \, \mathrm{m}^3$. In addition, through the on-site investigation of the

FIGURE 7 | The deposits and the bedrock after scraping are distributed in the landslide transportation area. **(B)** Landslide deposits at observation point D033. **(A,C)** There are many larger basaltic boulders in the upper part of landslide accumulation. **(E)** The material composition of the lower part of the landslide accumulation body is mainly composed of fine particles such as gravel and breccia. **(D,F)** The basaltic stones were mainly amygdaloidal and some show severe argillization. **(H)** Bedrock is exposed near survey point D015. **(G,I)** Scratches can be seen on the rock mass surface.

internal material composition of landslide accumulation at different locations, the debris deposit has the accumulation characteristics of inverse grading structure at different heights in the vertical profile of the landslide deposits. According to the research findings of scholars at home and abroad, many large-scale, high-speed, long-distance landslide debris flows show the accumulation characteristics of inverse grading structure in kinematics (Paola, 2000; Evans, 2006; Fan, 2019; Chen, 2021; Wu et al., 2021).

FORMATION MECHANISM OF THE JIAOPENBA LANDSLIDE

Landslide occurrence needs to go through three stages: deformation accumulation, triggering instability, and sliding failure.

Deformation Accumulation Process of Emeishan Basaltic Rock Mass

(1) Lithologic Composition Feature of Hard Rock and Intercalated Soft Rock

A large area of smooth bedding plane of limestone of Lower Permian Yangxin Formation (P_1Y) is exposed in the landslide source area, and parts of the unslided Emeishan Basaltic Rocks still exist at the trailing edge of the source area (**Figure 3**). Furthermore, according to the field investigation, most accumulations are composed of basalt blocks, and there exists no limestone component. It can be inferred that the sliding surface of the landslide is controlled by the weak intercalation of volcanic agglomerate and breccia at the bottom of Emeishan basalt (**Figure 11**).
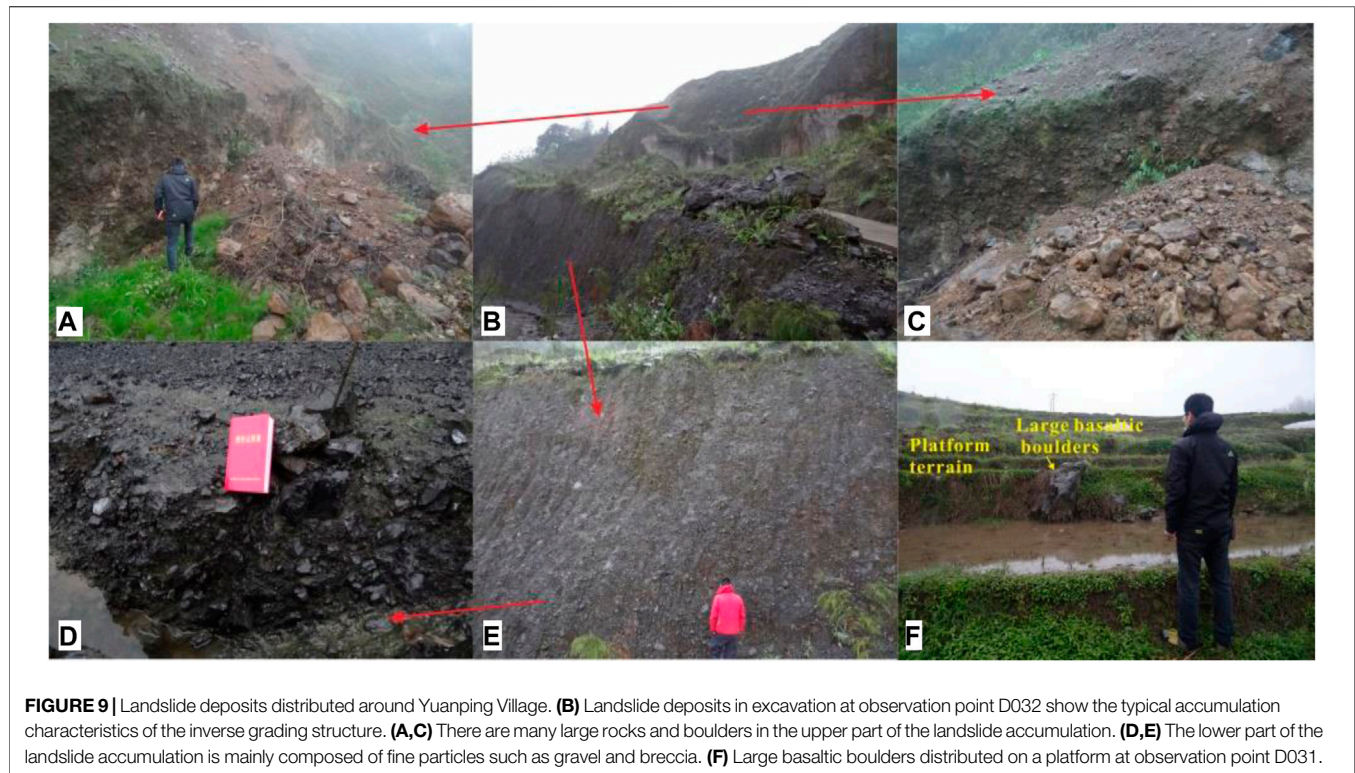
FIGURE 8 | Landslide deposits distributed around Qianchi Village. **(A)** Large basaltic boulders distributed at observation point D024. **(C)** The bedrock cover interface exposed at observation point D022. **(B)** Landslide deposits at the east side of the bedrock cover interface. **(D,E)** Large basaltic boulders distributed at observation point D025. **(F)** Landslide accumulation platform in Qianchi Village. **(G,H,I)** Landslide deposits at observation point D068.

During the condensation process of karst flow, primary columnar joints and layered joints parallel to the rock flow surface and perpendicular to the columnar joints are widely developed in Emeishan basalt (mainly including lithologic interface and eruption discontinuity formed by volcanic agglomerate, breccia layer, and tuff layer). The extensive development of layered joints makes basalt show a layered structure similar to sedimentary rock, which can often breed large-scale deformation and failure. In particular, volcanic agglomerates and breccias of the eruption discontinuity are mainly distributed at the bottom of each eruption cycle, with more pores, loose structure, and weak strength. These intercalations readily disintegrated and softened when wet, weakening the interlayer bonding within the rock mass, resulting in very low shear strength in the dip direction along the slope (**Figure 12A**).

(2) The Influence of Tectonic Reconstruction, Superficial and Epigene-Action

Although the shear outlet of the landslide is near the slope toe and does not have good free conditions, there are faults passing through the slope toe of the bedding slope of the fault hanging wall. The landslide is affected by the fault activity, and the integrity of the layered slope is poor (**Figure 13**). When the slope toe is free due to the continuous erosion of the river, the fault zone is compressed and plastic extrusion, which leads to bedding slip of the slope rock mass and greatly weakens the interlayer bonding force. When coupled with long structural planes on both sides to form side crack planes, a large-scale inclined plate structure is formed (**Figure 12B**). Therefore, the development of faults at the foot of the slope in the landslide source area played a controlling role in the formation of the shear outlet and the instability of the slope.

The deformation accumulation process of the Emeishan Basaltic rock mass is accompanied by the whole rock mass evolution process: the unique primary structural plane of Emeishan basalt makes the basaltic rock mass have a series of transverse and longitudinal staggered weak planes at the

FIGURE 9 | Landslide deposits distributed around Yuanping Village. **(B)** Landslide deposits in excavation at observation point D032 show the typical accumulation characteristics of the inverse grading structure. **(A,C)** There are many large rocks and boulders in the upper part of the landslide accumulation. **(D,E)** The lower part of the landslide accumulation is mainly composed of fine particles such as gravel and breccia. **(F)** Large basaltic boulders distributed on a platform at observation point D031.

beginning of diagenesis, which provides a potential fracture surface for the development of rock mass fragmentation. In the later stage, the rock mass was affected by tectonism and shallow epigenetic transformation. On the basis of primary formation, the structural plane further deformed and developed, and new fractures were generated. The rock mass structure further tended to be broken and cracked, and the saprolite crusts from chemical weathering occurred along discontinuity surfaces. Most of its mineral components have been transformed into clay minerals, soluble components, and other residual minerals, and the mechanical strength is closer to the soil. After a long-term deformation accumulation process, the Emeishan Basaltic rock mass has gradually changed from the original thick layered structure to the inclined plate structure and became an unstable slope body.

Triggering Instability Process of Emeishan Basaltic Rock Mass

The landslide accumulation area is distributed in the areas of Qianchi, Xianwan, Yuanping, and Nanmuping. Due to the accumulation of landslide materials and the erosion and undercutting of rivers in the later stage, the platform terrain separated by the river valley formed the fifth level planation plane in the study area (elevation: 900–1,000 m). Through the comparative analysis of regional planation levels and combined with the research results of Valley evolution in Dadu River Basin (Wang et al., 2013), it can be judged that the landslide was roughly formed in the Middle Pleistocene.

The thickness of the basalt stratum in the landslide area reaches tens of meters or even hundreds of meters, characterized by an extremely thick layered bedding rock slope. It is almost impossible for heavy rainfall to trigger such a large-scale landslide event. Through the study of seismic landslides, strong earthquake events in high earthquake intensity areas can often induce large-scale rock landslide events (Fan, 2019; Valagussa, 2019; Cui, 2020; Zhao, 2021a). The landslide area is located in the VII earthquake intensity area. According to the above analysis, the landslide is triggered by a strong earthquake event in the Middle Pleistocene, and the strong earthquake is the key factor causing the final sliding instability of the landslide (**Figure 12C**).

According to the theory of stress-wave propagation (Shen et al., 2019b; Hidayat et al., 2020; Luo et al., 2020; Zhao et al., 2021b; Hazarika et al., 2021), a compressional seismic wave will be reflected into a tensile wave when it meets a structural defect during propagation; this could increase the acceleration across the defect. As a result, tensile fractures may have formed as the reflected waves and incident waves were superposed. The seismic waves thus would have been magnified by the structural defects when the earthquake occurred, resulting in further tensional failure of the rock mass and tensile cracks in the upper part of the slope (**Figure 12C**).

Jiaopenba landslide developed in the hanging wall of the fault (**Figures 5**, **12**, **13**). The landslide is affected by fault activity, and the integrity of the layered slope is poor. When the foot of the slope was empty, the fault zone was compressed and plastically extruded, which led to bedding slip of the slope rock mass and greatly weakened the interlayer bonding force.
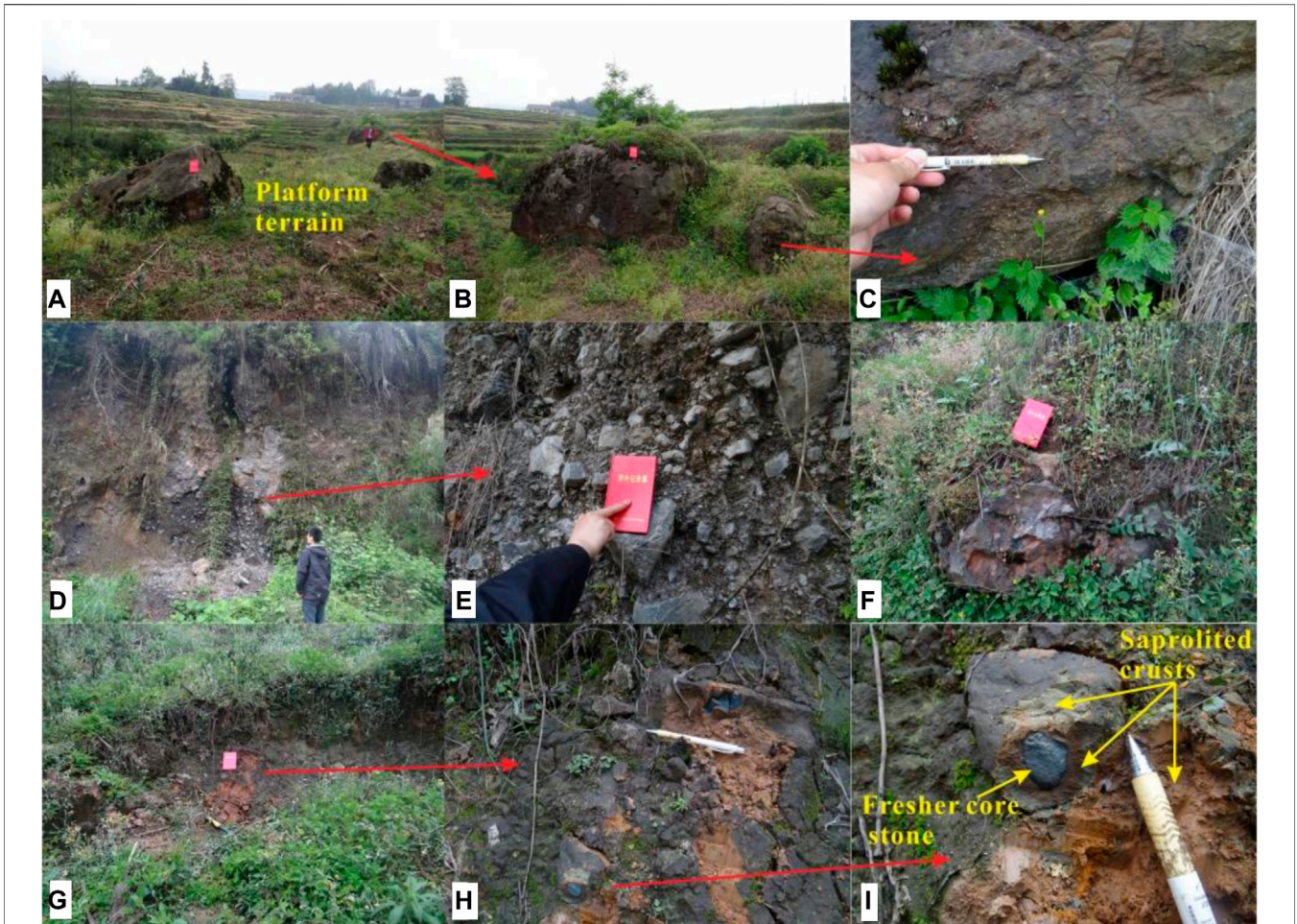
FIGURE 10 | Landslide deposits distributed around Nanmuping Village. (A,B,C) Large basaltic boulders distributed on a platform at observation point D046 (the basaltic blocks show severe argillization). (D,E,F) Landslide deposits at observation point D051. (G,H,I) Large basaltic boulders near observation point D051 are seriously weathered and present the structure of soil sandwiching rock.
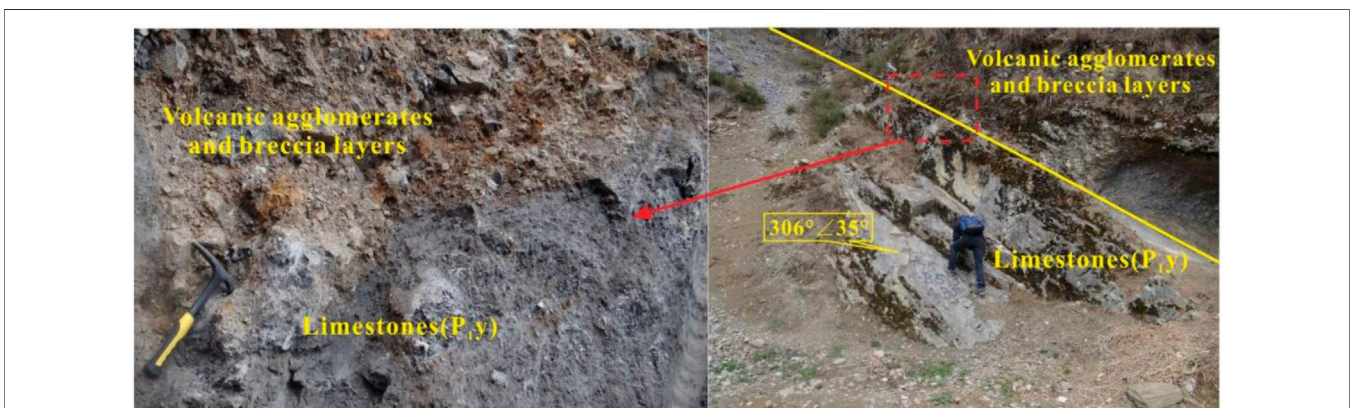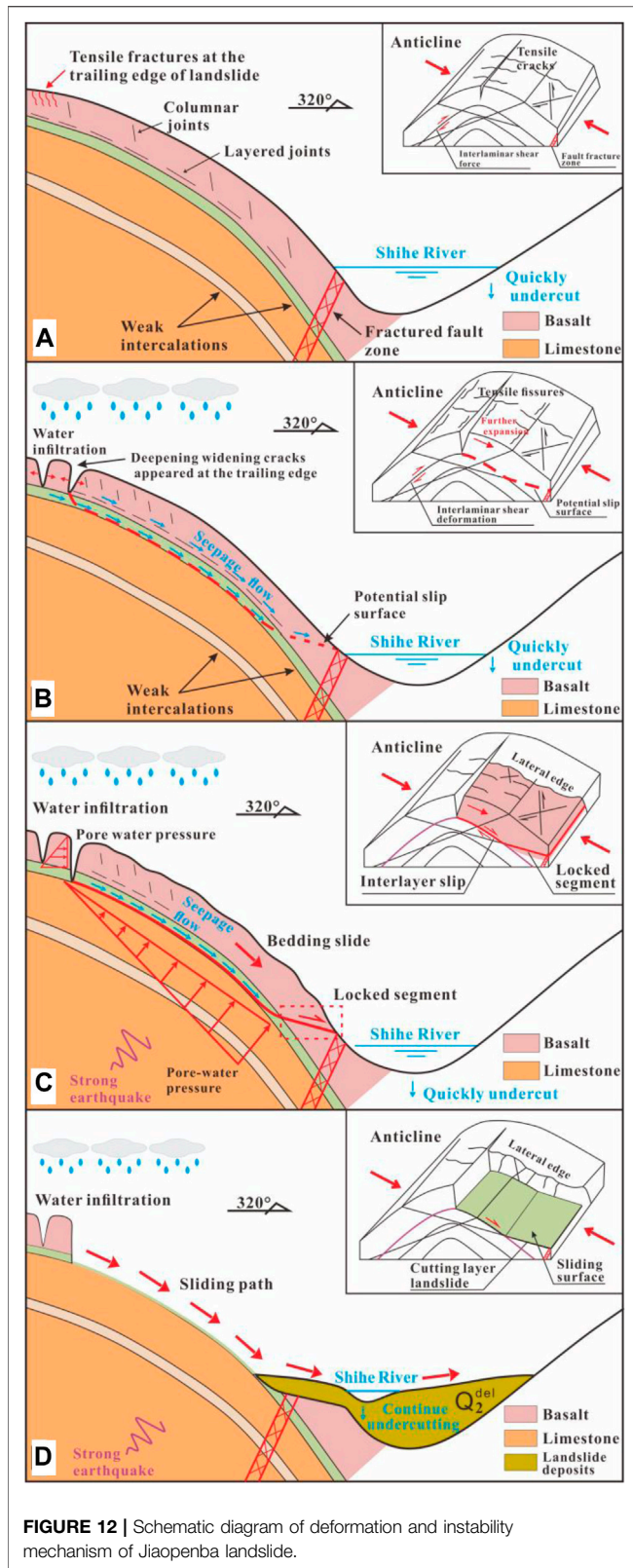

FIGURE 11 | The weak intercalation of volcanic agglomerates and breccias form the contact surface between basalt and underlying limestone (the photographing orientation is 340°).

FIGURE 12 | Schematic diagram of deformation and instability mechanism of Jiaopenba landslide.

When coupled with long structural planes on both sides to form side crack planes, a large-scale inclined plate structure was formed. Under the action of a strong earthquake, the rock mass near the fault can undergo tensile failure, forming a large high-position landslide in the mode of compression-slip-tension fracture (**Figure 12D**).

Long-Distance Sliding Mechanism of Emeishan Basaltic Rock Mass

Three key conditions are needed for the Jiaopenba landslide to maintain long-distance sliding.

(1) The Landslide Body Is at a High Position and Has a High Potential Energy

The elevation difference between the back edge of the slip source area and the front edge of the landslide area is 1,510 m, the height difference is huge, and the landslide body is in the high position of the slope, providing the sliding body with tremendous potential energy when sliding out of the shear outlet (**Figures 2**, **5**).

(2) Basaltic Rock Mass in Landslide Source Area Has a High Degree of Fragmentation

The size of broken blocks in the source area, confined by structural planes at all levels, plays a controlling role in the composition of debris size of the landslide accumulation and has a profound impact on the movement and evolution of the landslide.

The investigation of the particle size composition of 36 basalt landslide deposits in Southwest China reveals that the landslide materials are mainly coarse-grained debris (particle size > 2 mm), whereas the content of fine-grained components (particle size < 2 mm) is relatively small, and the clay particles are almost missing (particle size < 0.005 mm) (**Figure 14**). Therefore, the investigation shows that the Emeishan basalt debris flow is mainly composed of coarse-grained rocks. In the process of motion, large particles often collide with each other, with obvious momentum transfer so that they can slide farther (Wang, 2018; Ahmadipur, 2019; Wang, 2021).

(3) The Friction Energy Dissipation Between Particles Is Weak After the Landslide Body Starts to Move, and It Can Keep High-Speed Movement for a Long Time

Due to the high degree of development and uniform distribution of structural planes of basaltic rock mass, the sphericity of clastic particles after crushing structural bodies surrounded by structural planes is often better. Sphericity refers to the similarity between the shape of debris particles and spheres. Sphericity reflects the shape of particles in three-
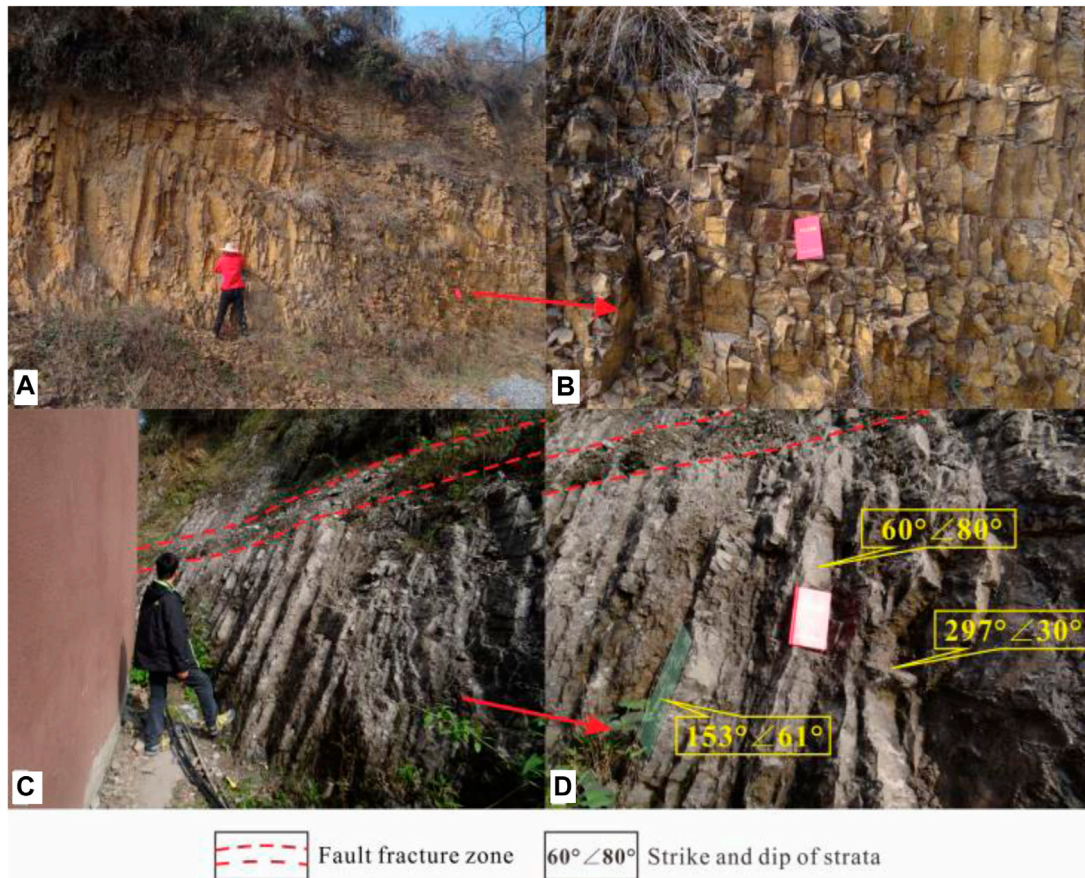
FIGURE 13 | Basaltic bedrock is exposed in the landslide source. **(A)** Columnar joints are developed in basaltic rocks. **(B)** The degree of rock fragmentation and cracking is high. **(C)** Fault fracture zone is exposed near the shear outlet of the landslide. **(D)** The attitude of bedrock in the source area.
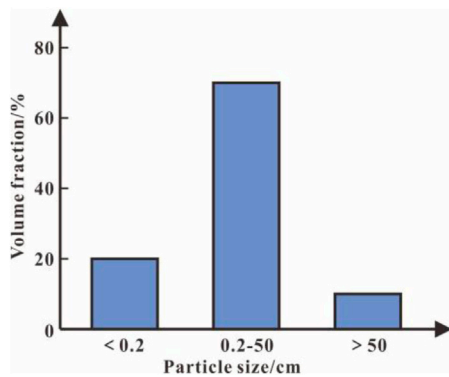

FIGURE 14 | Statistics of particle size composition of basalt landslide deposits in Southwest China.

dimensional space. Generally, the sphericity coefficient is calculated by the formula proposed by Krubin (1941):
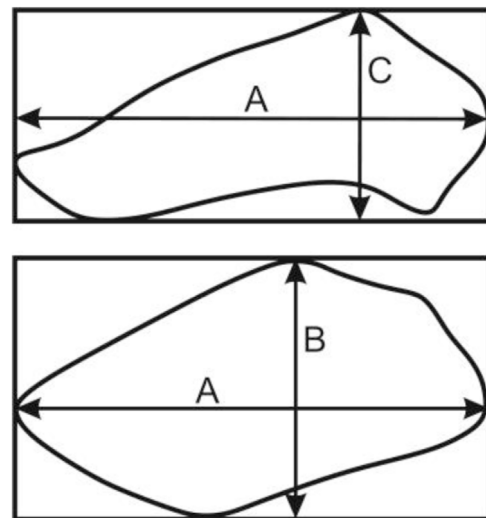
$$\varnothing = \sqrt[3]{BC/A^2}, \qquad (1)$$

FIGURE 15 | Schematic diagram of the position of A, B, and C axes of debris particles (the upper part is the sectional view of debris particles, and the lower part is the plan view).

TABLE 1 | Sphericity investigation of basalt clastic particles.

Investigation points	Number	Particle diameter (cm)			Sphericity coefficient ∅	Proportion of particles with good sphericity (%)
		A	B	C		
D032	1	12.3	5.6	3.6	0.51	60
	2	5	4.5	3.7	0.87	
	3	11	5.1	2.6	0.48	
	4	4.8	4	3.2	0.82	
	5	6.4	4.8	2.5	0.66	
	6	5.2	3.9	2.5	0.71	
	7	3.1	2.6	1.2	0.69	
	8	2.7	2	1.6	0.76	
	9	3.8	3.5	3.2	0.92	
	10	4	2.6	1.1	0.56	
	11	2.2	1.5	0.8	0.63	
	12	7.5	2.4	1	0.35	
	13	8	5.1	3	0.62	
	14	8.6	6.1	3.6	0.67	
	15	5.5	2	0.9	0.39	
	16	2.8	1.5	0.7	0.51	
	17	2.3	1.6	1.3	0.73	
	18	5.8	2.9	1.3	0.48	
	19	3.6	2.3	1.9	0.7	
	20	12.2	5.8	5.1	0.58	
	21	8.3	6.8	5	0.79	
	22	1.9	0.8	1	0.61	
	23	6	1.9	0.8	0.35	
	24	2.5	2	1.7	0.81	
	25	10	7.9	5.2	0.74	
	26	5.1	1.2	0.7	0.32	
	27	7.6	7	5.6	0.88	
	28	3	1.5	1	0.55	
	29	9.2	7.2	6.9	0.84	
	30	6.7	3.3	1.5	0.48	
D033	1	8	6.7	4.1	0.75	67
	2	4.9	3	1.3	0.55	
	3	4.3	2.1	0.7	0.43	
	4	20.7	10.6	10.3	0.63	
	5	10.2	7.5	5	0.71	
	6	6.3	5.9	5.2	0.92	
	7	5.1	3.2	0.8	0.46	
	8	8.3	5.2	4.2	0.68	
	9	6.6	3.4	0.8	0.4	
	10	9.1	8.3	6.2	0.85	
	11	8.5	5.4	1.9	0.52	
	12	11.6	10.6	4.8	0.72	
	13	5.6	3.2	2.8	0.66	
	14	7.5	6.8	3.6	0.76	
	15	5	4.1	2	0.69	
	16	13.7	10.9	6.8	0.73	
	17	4	3.1	2.1	0.74	
	18	3.2	2	1	0.58	
	19	15.2	11.3	6.7	0.69	
	20	6.5	2.6	0.9	0.38	
	21	4.8	3	1.7	0.6	
	22	5	3.1	1.1	0.51	
	23	5.3	3.9	1.8	0.63	
	24	18.1	17.6	12.8	0.88	
	25	13.6	8.1	2	0.44	
	26	7.7	6	4.9	0.79	
	27	8.5	7.9	6.9	0.91	
	28	5.2	3.4	2.1	0.64	
	29	9.6	7.1	2.4	0.57	
	30	6.4	5.3	4.6	0.84	

TABLE 1 | (*Continued*) Sphericity investigation of basalt clastic particles.

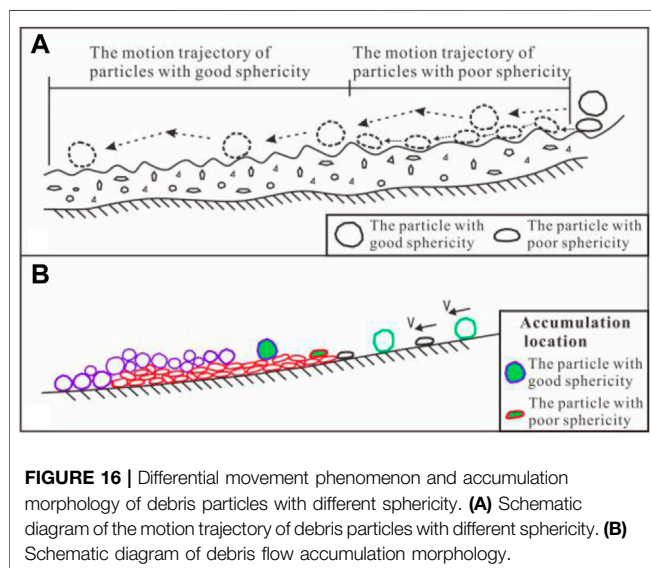| Investigation points	Number	Particle diameter (cm)			Sphericity coefficient ∅	Proportion of particles with good sphericity (%)
		A	B	C		
D051	1	4.1	1.5	0.5	0.35	53
	2	1.3	0.9	0.5	0.64	
	3	3.7	2.2	1.1	0.56	
	4	3	1.5	0.4	0.41	
	5	2.8	2.3	1.7	0.79	
	6	3.4	1.2	0.5	0.37	
	7	5.9	5.5	4.8	0.91	
	8	8.2	4.8	2.3	0.55	
	9	6.3	4.1	3.6	0.72	
	10	1.5	1.2	0.5	0.64	
	11	2.4	1.6	0.5	0.52	
	12	4.3	3.2	1.9	0.7	
	13	3.9	1.7	1	0.48	
	14	7.9	6.7	6.2	0.87	
	15	5.3	2.5	1.3	0.49	
	16	5.5	3.4	1.8	0.59	
	17	9.4	6.8	5.1	0.73	
	18	6	5	4.5	0.85	
	19	1.9	1.2	0.4	0.51	
	20	2.1	1.9	0.7	0.67	
	21	6	1.8	1.2	0.39	
	22	5.6	4.8	3.1	0.78	
	23	3.7	1.3	0.6	0.38	
	24	2.9	2.5	2.3	0.88	
	25	4.2	1.6	1.1	0.46	
	26	7.1	4.4	2.7	0.62	
	27	2.8	0.6	0.4	0.31	
	28	4.8	3.9	3	0.8	
	29	6.5	6.1	5.6	0.93	
	30	3.4	2.6	1.4	0.68	

FIGURE 16 | Differential movement phenomenon and accumulation morphology of debris particles with different sphericity. **(A)** Schematic diagram of the motion trajectory of debris particles with different sphericity. **(B)** Schematic diagram of debris flow accumulation morphology.

plane. The three axes *A*, *B*, and *C* are perpendicular to each other in space but do not necessarily intersect at one point (**Figure 15**).

The sphericity of debris particles was investigated at the Jiaopenba landslide accumulation area. The survey points were D032, D033, and D051 (the locations of the survey points are shown in **Figures 2**, **7**, **9**, **10**). At each survey site, a measurement area was randomly selected. According to the calculation formula of the Krubin sphericity coefficient, 30 debris particles were randomly selected in the measurement area to calculate their sphericity. Finally, the sphericity coefficients of each debris particle were statistically summarized (**Table 1**). Results indicate that the basalt debris particles with a higher degree of fracture have better particle sphericity (the proportion of debris particles with sphericity above 0.6 in the study area is about 60%), and particles with good sphericity are prone to bounce and roll during movement (**Figure 16**). Under this movement mode, the effective friction coefficient between particles and sliding surface is lower and has a momentum transfer effect during the movement, so that the basalt debris particles exhibit stronger mobility and thus can slide further distances, and then the scope of the landslide will be even greater.

After long-term weathering, the basaltic rock mass in the landslide source area becomes saprolite crusts with a layered structure. Most of its mineral components have been transformed

where ∅ is the sphericity coefficient, *A* is the maximum diameter on the largest space plane of the particle, B is the maximum diameter perpendicular to axis *A* on the largest space plane, and *C* is the maximum diameter perpendicular to the largest space

FIGURE 17 | Basaltic rocks present the structure the structure of soil sandwiching rock due to severe weathering.

TABLE 2 | Physical and hydraulic property indexes of weathered basalt (Wang, 2013).

Rock mass structure	Density (g/cm^3)	Porosity (%)	Permeability (×10^{-3}μm^2)
The external saprolite crusts	1.8816	32.82	301.5157
The inner fresher core stone	2.9434	0.24	0.0081

into clay minerals, soluble components, and other residual minerals. The external saprolite crusts crumble as soon as it is pinched, and their mechanical strength is almost lost (**Figure 17**, **Table 2**). Therefore, after the unstable sliding of the rock mass, the external saprolite crusts quickly break into fine particles, scatter around the inner fresher core stone, and act as a "lubricant."

Moreover, the landslide body passed through a far valley section in the process of sliding. Due to the existence of quaternary deposits with higher water content around Shihe River, it also plays a certain role in lubricating the movement of landslide materials. The comprehensive effect of the above factors makes the landslide debris flow maintain a higher speed and a longer distance.

CONCLUSION

The Jiaopenba landslide was a giant basalt high-speed landslide debris flow induced by a combination of factors, probably including strong earthquake ground shaking. The landslide occurred on the

steep Mount Emei, with a volume of approximately 6.75×10^8 m^3 slid down from a high position along a surface formed by weak intercalation of volcanic agglomerate and breccia, and the farthest sliding distance reached about 7.5 km.

On the basis of primary formation, the basalt was affected by tectonism and shallow epigenetic transformation, and its structural plane further deformed and developed, resulting in new fractures. The saprolite crusts from chemical weathering developed along discontinuity surfaces, and most of the mineral components have been transformed into clay minerals, soluble components, and other residual minerals, and their strength is closer to the soil. After a long-term deformation accumulation process, the basaltic rock mass has gradually changed from the original thick layered structure to the inclined plate structure and became an unstable slope body.

Jiaopenba landslide developed in the hanging wall of the fault. When the slope toe was empty, the fault zone was compressed and plastically extruded, which led to bedding slip of the slope rock mass and greatly weakened the interlayer bonding force. When coupled with long structural planes on both sides to form side crack planes, a

large-scale inclined plate structure was formed. Under the action of a strong earthquake, the rock mass near the fault can undergo tensile failure, forming a large high-position landslide in the mode of compression-slip-tension fracture.

The basalt debris flow is mainly composed of coarse-grained rocks. In the process of motion, large particles often collide with each other, with an obvious momentum transfer effect. In addition, the basalt debris particles with a higher degree of fracture have better particle sphericity, which are prone to bounce and roll during movement. Under this movement mode, the effective friction coefficient between particles and the sliding surface is lower. The combination of factors makes the landslide debris flow maintain a higher speed and a longer distance.

DATA AVAILABILITY STATEMENT

The datasets presented in this study can be found in online repositories. The names of the repository/repositories and accession number(s) can be found in the article/supplementary material.

AUTHOR CONTRIBUTIONS

TS and YW were responsible for writing. XZ provided engineering data and geophysical analysis of the slope. HL, XW, and YC analyzed the deformation and failure characteristics of the slope. PZ and YH were responsible for review and proofreading.

FUNDING

REFERENCES

Ahmadipur, A., Qiu, T., and Sheikh, B. (2019). Investigation of Basal Friction Effects on Impact Force from a Granular Sliding Mass to a Rigid Obstruction. *Landslides* 16 (6), 1089–1105. doi:10.1007/s10346-019-01156-0

Chen, J., Chen, R. C., and Cui, Z. J. (2021). Research Progress on the Morphology and Sedimentology of Long Runout Landslide. *Earth Sci. Front.* 28 (4), 349–360. doi:10.13745/j.esf.sf.2020.7.2

Cui, S., Yang, Q., Pei, X., Huang, R., Guo, B., and Zhang, W. (2020). Geological and Morphological Study of the Daguangbao Landslide Triggered by the Ms. 8.0 Wenchuan Earthquake, China. *Geomorphology* 370, 107394. doi:10.1016/j.geomorph.2020.107394

Evans, S. G., Mugnozza, G. S., Strom, A. L., Hermanns, R. L., Ischuk, A., and Vinnichenko, S. (2006). Landslides from Massive Rock Slope Failure and Associated Phenomena. *Landslides* 49, 03–52. doi:10.1007/978-1-4020-4037-5_1

Fan, X., Scaringi, G., Korup, O., West, A. J., Westen, C. J., Tanyas, H., et al. (2019). Earthquake-Induced Chains of Geologic Hazards: Patterns, Mechanisms, and Impacts. *Rev. Geophys.* 57 (2), 421–503. doi:10.1029/2018rg000626

Han, G. (2015). *A Type of Asymmetric Distributed Deep-Seated Crack Formation Mechanism: A Case Study of Baihetan Hydropower Station*. Chengdu: Doctoral Dissertation of Chengdu University of Technology. in Chinese.

Hazarika, H., Rohit, D., Pasha, S. M. K., Maeda, T., Masyhur, I., Arsyad, A., et al. (2021). Large Distance Flow-Slide at Jono-Oge Due to the 2018 Sulawesi Earthquake, Indonesia. *Soils Found.* 61 (1), 239–255. doi:10.1016/j.sandf.2020.10.007

Hidayat, R. F., Kiyota, T., Tada, N., Hayakawa, J., and Nawir, H. (2020). Reconnaissance on Liquefaction-Induced Flow Failure Caused by the 2018 Mw 7.5 Sulawesi Earthquake, Palu, Indonesia. *J. Eng. Technol. Sci.* 52 (1), 51–65. doi:10.5614/j.eng.technol.sci.2020.52.1.4

Luo, Y., Fan, X., Huang, R., Wang, Y., Yunus, A. P., and Havenith, H. B. (2020). Topographic and Near-Surface Stratigraphic Amplification of the Seismic Response of a Mountain Slope Revealed by Field Monitoring and Numerical Simulations. *Eng. Geol.* 271, 105607. doi:10.1016/j.enggeo.2020.105607

Paola, C. (2000). Sedimentology and Sedimentary Basins: from Turbulence to Tectonics. *Nature* 405, 171–197. doi:10.1038/35012122

Shen, T. (2019). *Formation Mechanism of Large-Scale High-Position and Long-Distance Landslide in Emeishan Basalt*. Chengdu: Doctoral Dissertation of Chengdu University of Technology. in Chinese.

Shen, T., Wang, Y., Huang, Z., Li, J., Zhang, X., Cao, W., et al. (2019a). Formation Mechanism and Movement Processes of the Aizigou Paleolandslide, Jinsha River, China. *Landslides* 16 (2), 409–424. doi:10.1007/s10346-018-1082-1

Shen, T., Wang, Y.-s., Luo, Y.-h., Xin, C.-c., Liu, Y., and He, J.-x. (2019b). Seismic Response of Cracking Features in Jubao Mountain during the Aftershocks of Jiuzhaigou Ms7.0 Earthquake. *J. Mt. Sci.* 16 (11), 2532–2547. doi:10.1007/s11629-019-5570-0

Sun, S. Q. (2011). *Study on the Types of Rock Mass Structural Planes and Engineering Effect in Emeishan Basalt*. Chengdu: Doctoral Dissertation of Chengdu University of Technology. in Chinese.

Tian, Y. Y., Xu, C., Xu, X. W., Wu, S. E., and Chen, J. (2015). Spatial Distribution Analysis of Coseismic and Pre-earthquake Landslides Triggered by the 2014 Ludian Ms 6.5 Earthquake. *Seismol. Geol.* 37 (1), 291–306. doi:10.3969/j.issn.0253-4967.2015.01.023

Valagussa, A., Marc, O., Frattini, P., and Crosta, G. B. (2019). Seismic and Geological Controls on Earthquake-Induced Landslide Size. *Earth Planet. Sci. Lett.* 506, 268–281. doi:10.1016/j.epsl.2018.11.005

Wang, P. (2013). *Fragmentation Mechanism of Original Rock Mass in Touzhai Landslide*. Kunming: Master's thesis of Kunming University of Science and Technology. in Chinese.

Wang, Y. S., Wang, D. P., Wang, J. Z., Fu, R. H., and Yang, Y. N. (2013). Study on the Formation of the Emei Faulty Bock Mountain. *South-to-North Water Transfers Water Sci. Technol.* 11 (1), 110–113. doi:10.3724/SP.J.1201.2013.01110

Wang, Y. F., Dong, J. J., and Cheng, Q. G. (2018). Normal Stress-dependent Frictional Weakening of Large Rock Avalanche Basal Facies: Implications for the Rock Avalanche Volume Effect. *J. Geophys. Res. Solid Earth* 123 (4), 3270–3282. doi:10.1002/2018JB015602

Wang, Y. F., Lin, Q. W., Li, K., Shi, A. W., Li, T. H., and Cheng, Q. G. (2021). Review on Rock Avalanche Dynamics. *J. Earth Sci. Environ.* 43 (1), 164–181. doi:10.19814/j.jese.2020.10001

Wei, Y. J., Chu, H. L., Zhuang, M. G., Wang, C. F., and Bai, Y. Y. (2016). Formation Mechanism of Wangshan-Zhuakousi Landslide in Emei City, Sichuan Province. *J. Eng. Geol.* 24 (3), 476–483. doi:10.13544/j.cnki.Jeg.2016.03.018

Wei, Y. J. (2007). *Study on Characteristics of Rock Mass Structure and Engineering Application of Emeishan Basalts in Project Site of Hydroelectric Power Station in Southwest China*. Chengdu: Doctoral Dissertation of Chengdu University of Technology. in Chinese.

Wen, B. P., and Wang, F. (2021). Precursors and Motion Characteristics of the 1965 Lannigou Rockslides and the Subsequent Evolution. *Hydrogeology Eng. Geol.* 48 (6), 72–80. doi:10.16030/j.cnki.issn.1000-3665.202108065

Wu, H., Pei, X. J., Cui, S. H., Huang, R. Q., and Song, C. (2021). Study of Topographic and Geological Controls on Landslide Development and Distribution within Mountainous Regions Influenced by Strong Earthquakes. *Chin. J. Rock Mech. Eng.* 40 (5), 972–986. doi:10.13722/j.cnki.jrme.2020.0944

Xu, Z. M., Huang, R. Q., and Tang, Z. G. (2005). Kinetics of Silicate Mineral Dissolution and its Implications for Landslide Studies. *Chin. J. Rock Mech. Eng.* 24 (09), 1479–1491. in Chinese.

Xu, Q., Dong, X. J., Deng, M. L., Chen, L., and Hu, Z. M. (2010). The Ermanshan Rock Slide-Debris Flow of July 27, 2010 in Hanyuan, Sichuan: Characteristics and Failure Mechanism. *J. Eng. Geol.* 18 (5), 609–622. in Chinese.

Yang, J.-q., Xu, Z.-m., Zhang, R., Chen, J.-p., Ren, Z., Luo, R.-z., et al. (2017). Formation and Evolution of Emeishan Basalt Saprolite in Vadose Zones of Touzhai Landslide Source Rockmass. *J. Mt. Sci.* 14 (6), 1174–1184. doi:10.1007/s11629-016-4169-y

Zhang, X. S. (2017). *Expansion Mechanism of Weathering Front of Rock Blocks with Low Permeability in Slope Unsaturated Zone*. Kunming: Master's thesis of Kunming University of Science and Technology. in Chinese.

Zhao, B., Su, L., Wang, Y., Ji, F., Li, W., and Tang, C. (2021a). Insights into the Mobility Characteristics of Seismic Earthflows Related to the Palu and Eastern Iburi Earthquakes. *Geomorphology* 391, 107886. doi:10.1016/j.geomorph.2021.107886

Zhao, B., Wang, Y., Wu, J., Su, L., Liu, J., and Jin, G. (2021b). The Mogangling Giant Landslide Triggered by the 1786 Moxi M 7.75 Earthquake, China. *Nat. Hazards* 106, 459–485. doi:10.1007/s11069-020-04471-1